LM-04K047
June 9, 2004

0.52eV Quaternary InGaAsSb Thermophotovoltaic Diode Technology

M.W. Dashiell, J.F. Beausang, G. Nichols, D.M. Depoy, L.R. Danielson, H. Ehsani, K.D. Rahner, J. Azarkevich, P. Talamo, E. Brown, S. Burger, P. Fourspring, W. Topper, P.F. Baldasaro, C.A. Wang, R. Huang, M. Connors, G. Turner, Z. Shellenbarger, G. Taylor, Jizhong Li, R. Martinelli, D. Donetski, S. Anikeev, G. Belenky, S. Luryi, D.R. Taylor and J. Hazel

0.52 eV Quaternary InGaAsSb Thermophotovoltaic Diode Technology

M.W. Dashiell[a], J.F. Beausang[a], G. Nichols[a], D.M. Depoy[a], L.R. Danielson[a], H. Ehsani[a], K.D. Rahner[a], J. Azarkevich[a], P. Talamo[a], E. Brown[a], S. Burger[a], P. Fourspring[a], W. Topper[a], P.F. Baldasaro[a], C.A. Wang[b], R. Huang[b], M. Connors[b], G. Turner[b], Z. Shellenbarger[c], G. Taylor[c], Jizhong Li[c], R. Martinelli[c], D. Donetski[d], S. Anikeev[d], G. Belenky[d] and S. Luryi[d], D.R. Taylor[e], J. Hazel[e]

[a]*Lockheed Martin Corporation, Schenectady, New York 12301-1072*
[b]*MIT Lincoln Laboratory, Lexington Massachusetts 02420-9108*
[c]*Sarnoff Corporation, Princeton, New Jersey 08543-5300*
[d]*State University of New York, Stony Brook, New York 11794-2350*
[e]*Bandwidth Semiconductor, Hudson, New Hampshire 03051*

Abstract. Thermophotovoltaic (TPV) diodes fabricated from 0.52eV lattice-matched InGaAsSb alloys are grown by Metal Organic Vapor Phase Epitaxy (MOVPE) on GaSb substrates. 4cm^2 multi-chip diode modules with front-surface spectral filters were tested in a vacuum cavity and attained measured efficiency and power density of 19% and 0.58 W/cm^2 respectively at operating at temperatures of $T_{radiator}$ = 950 °C and T_{diode} = 27 °C. Device modeling and minority carrier lifetime measurements of double heterostructure lifetime specimens indicate that diode conversion efficiency is limited predominantly by interface recombination and photon energy loss to the GaSb substrate and back ohmic contact. Recent improvements to the diode include lattice-matched p-type AlGaAsSb passivating layers with interface recombination velocities less than 100 cm/s and new processing techniques enabling thinned substrates and back surface reflectors. Modeling predictions of these improvements to the diode architecture indicate that conversion efficiencies from 27-30% and ~0.85 W/cm^2 could be attained under the above operating temperatures.

INTRODUCTION

Thermophotovoltaic (TPV) converters have attracted interest in the field of direct energy conversion due to the potential for relatively high efficiency operation with no moving parts. For hot side temperatures of less than 1500^{o}C, greater than 20% thermal to electric efficiency requires: (i) Efficient spectral control that reflects below-bandgap photons back to the radiator and transmits above-bandgap photons to the diode[1] and (ii) efficient photovoltaic conversion of above-bandgap photons to electric power. The highest reported thermal to electric TPV efficiencies, 22% for the 0.6eV InGaAs/InP[2] and 19% for 0.52eV InGaAsSb/GaSb material systems, both utilize a front surface plasma/interference filter mounted to the TPV module[2]. Radiator and diode temperatures are taken to be 950°C and diode temperature of 27°C unless otherwise noted. While 0.6 eV InGaAs diode grown on InPAs buffers and an InP substrate have demonstrated the record conversion efficiency, the InGaAsSb material offers a lattice-matched alternative grown on a GaSb substrate. Currently, development work of ~0.5eV InGaAs/InP[3] and InGaAsSb/GaSb[4-6] TPV materials is ongoing due to the greater power density expected from 0.5eV TPV material. This work discusses theoretical predictions of TPV conversion efficiencies at the small module level of 27 to 30% with power densities of ~0.8-0.9 W/cm^2 and the status of device fabrication and material growth/characterization that has been developed to achieve these predictions. Modeling indicates that the optimum 0.52eV TPV diodes operates with minimal dopant near the intrinsic Auger limit and requires negligible defect recombination and a back surface reflector for effective photon recycling and two pass architecture.

THEORY AND ASSUMPTIONS

The analysis presented here illustrates the limiting effect of Auger recombination on TPV diode conversion efficiency, and the competing influences of poor photon recycling and defect-assisted recombination. Auger recombination of photogenerated carriers sets a fundamental limit to conversion efficiency below the thermodynamic limit, which is determined by the radiative heat transfer between the radiator and diode of a given bandgap.[7,8] Auger coefficients for low bandgap III-V materials (0.5-0.6eV) have recently been measured via minority carrier lifetime in the range of $1x10^{-28}cm^6/s$[9,10].

The thermal to electric conversion efficiency of TPV is equal to the diode efficiency (electric output power to the above-bandgap radiation absorbed in the diode) multiplied by the spectral efficiency (above-bandgap radiation absorbed in the diode to the total heat absorbed at the cold side). The optimal diode bandgap, when considering 95-97% reflection of all below-bandgap photons is in the range of 0.5 to 0.6eV[1] for a 950°C radiator. Figure 1 shows the measured reflection and absorption of today's 0.52eV front surface filter technology[11] corresponding to 80% spectral efficiency. Figure 1 also shows an idealized step function reflection assumed for the modeling in this work(dashed lines). The radiator is also assumed to have a uniform emissivity of 0.9. The familiar effective emissivity equation for infinite parallel plates is given as equation (1):

$$e_{eff} = \frac{1}{\frac{1}{e_{radiator}} + \frac{1}{e_{diode}} - 1} = \frac{1}{\frac{1}{0.9} + \frac{1}{1 - R(l)} - 1} = \begin{cases} 0.78, & l < l_{Eg} \\ 0.03, & l > l_{Eg} \end{cases} \quad (1)$$

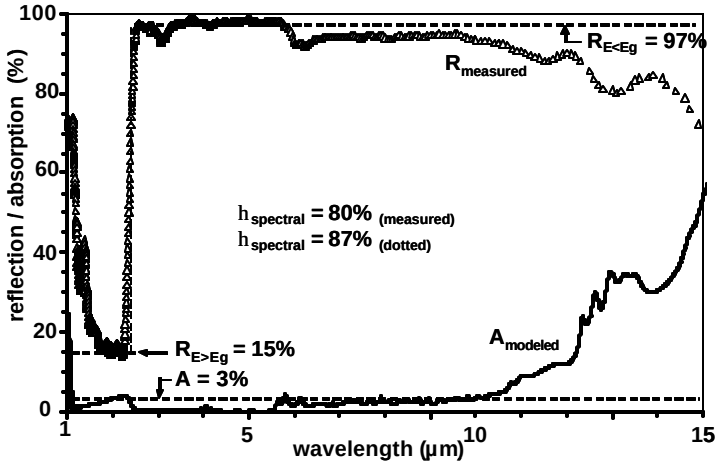

FIGURE 1. Angle-of-incidence (θ = 11°, 30°, 45°, 60° and 80°) weighted filter reflectance (triangles) designed for glue adhesive, but measured in air[11]. Filter absorption (solid) is calculated for the actual filter design with OptiLayer software. Measured above band gap transmission of filters is 79% and spectral efficiency is 80%. The performance projections in the modeling studies of this paper assume a step function reflectance (15% to 97%) and 3% absorption (87% spectral efficiency).

These effective emissivity and reflection values assumed in the equation (1) correspond to an 87% spectral efficiency for a 950°C radiator. The integrated above-bandgap transmissivity (T) includes the effective cavity emissivity, as wells as, above-bandgap absorption in the filter and is equal to T=79%. Thus maximum short-circuit current density for the 0.52 eV device and 950 °C radiator considered here is 3.6 A/cm^2 .

For the remainder of the discussion, the focus is on the diode efficiency, which can be expressed in terms of the following four parameters (FF = fill factor, QE = quantum efficiency, F_o = overexcitation factor, and qV_{oc}/E_g = voltage factor, see reference [1]).

$$h_{diode} = QE \cdot F_o \cdot FF \cdot {qV_{oc}}/{E_G} \quad (2)$$

0.52eV InGaAsSb TPV diodes routinely demonstrate high fill factors of 70%, high QE[12], and a fixed overexcitation factor of 0.78 for a 950°C radiator. The limit to open-circuit voltage in a photovoltaic diode, V_{OC}, is set by the maximum electrochemical potential energy generated under illumination due to the steady-state concentration of electron-hole pairs generated in the diode material. In ideal diode material, with only radiative recombination and no parasitic absorption losses to the back contact, the maximum steady-state electrochemical potential in the diode, corresponds to the diode-emitted photon flux required to balance the absorbed photon flux.[1,13,14] In an actual diode, however, the electrochemical potential will be less than this thermodynamic limit due to non-radiative recombination in the diode and reduced photon recycling with a partially absorbing back contact/substrate.

The reduction in maximum voltage due to non-radiative recombination is analyzed using a simple architecture following that of references [7,8]. The architecture assumes light is generated in an absorbing p-type volume of width W and a thin n-type region that absorbs negligible light (i.e., the diode is a one-sided abrupt junction). An implicit assumption is that the minority-carrier diffusion length is much larger than the width of the absorbing region (i.e., high minority carrier mobility). The simple expressions provide useful bounds for more thorough one-dimensional numerical simulations discussed in section 2.4. Under these simplified assumptions, the relation between the open-circuit voltage and the electron-hole density for a non-degenerate semiconductor is given by

$$np = n_i^2 \exp\left(\frac{qV_{OC}}{kT_{diode}}\right) \quad (3)$$

where n and p are the electron and hole densities, n_i is the intrinsic carrier concentration of the material, q is the electronic charge, k is Boltzmann's constant, and V_{OC} is the open-circuit voltage. At 27°C n_i is 7×10^{13} cm^{-3} for 0.52eV InGaAsSb as determined via linear interpolation of the binary alloy components.

Under open-circuit voltage, the steady-state continuity equation under illumination will determine the voltage in terms of the light generated current and is thus valid for both high and low level injection[8,16]. High-level injection refers to the regime where the photogenerated carrier concentration (Δn or Δp) is comparable to the dopant density (N_D or N_A), whereas low-level injection refers to the regime where $\Delta n << N_D$ or $\Delta p << N_A$. Low-level injection is a common assumption as it simplifies analysis since only one type of carrier dictates performance. Unfortunately, this simplification cannot accurately predict optimized diodes that are limited by Auger recombination of photogenerated carriers.

THERMODYNAMIC LIMIT TO OPEN-CIRCUIT VOLTAGE

In terms of radiative recombination rates, the thermodynamic limit to open-circuit voltage as a function of light generated current can be calculated from equations (2-4) via the Schockley van Rooesbroeck equation[16] using optical/electrical constants for 0.52eV InGaAsSb and the photon recycling factor calculated via Asbeck's method[17]. The thermodynamic limit to open-circuit voltage for the stated operating temperatures, and 0.52 eV bandgap is 420mV (at J_L = 3.6 A/cm^2 / T_{rad}=950°C). In comparison, the radiative limit for the same diode with an absorbing back contact is 370mV due to the ~ n_r^2 (n_r is the index of refraction of the substrate) increase in radiative dark current[14].

AUGER LIMIT TO OPEN-CIRCUIT VOLTAGE

Auger recombination, unlike radiative recombination is an irreversible process, in that the recombination energy is lost as heat, whereas radiative events can be reabsorbed. The Auger recombination rate per unit volume (U_{Auger}) is given by:

$$U_{Auger} = C_n n^2 p + C_p n p^2 \quad (4)$$

Where C_n and C_p are the Auger coefficients in units of cm^6/s. The total carrier densities n and p depend upon the ionized dopant density (N_A and N_D) and the excess electron-hole concentrations due to photogeneration ($\Delta p = \Delta n$). For a p-type semiconductor in low-injection ($\Delta n << N_A$) the net Auger recombination rate can be reduced by lowering the background doping density, however, as the background carrier density approaches the excess carrier density ($\Delta p \approx N_A$) the absorbing region enters high-level injection, where the excess carriers dictate the minimum Auger recombination rate and thus optimum performance below the thermodynamic limit.

Determining the Auger-limited Voc from equations (2, 3, and 4) requires the solution of a cubic expression for carrier density as a function of doping (N_A), light generated current (J_L), thickness (W), and the Auger recombination coefficients. At the asymptotic limits of very low-level (LLI) and very high-level injection (HLI) simplified expressions for the Auger-limited V_{OC} can be expressed[8]:

$$V_{OC}^{Auger-LLI} = \frac{kT}{q} ln\left(\frac{J_L}{q n_i^2 N_A C_p W}\right) \quad , \quad V_{OC}^{Auger-HLI} = \frac{2}{3}\frac{kT}{q} ln\left(\frac{J_L}{q n_i^3 (C_n + C_p) W}\right) \quad (5\text{-}6)$$

Assuming an ambipolar Auger coefficient of $1\times10^{-28} cm^6/s$, the intrinsic Auger limit(high-level injection limit) to open-circuit voltage in a 2.5μm thick 0.52eV InGaAsSb diode with a light generated current of 3 A/cm^2 is 360 mV. It is important to note that the Auger recombination significantly decreases the efficiency potential of a TPV diode below the thermodynamic limit discussed in section 2.1. For diodes with an absorbing back surface Auger recombination and the increased radiative losses contribute similarly to the parasitic heat transfer:

$$\begin{aligned} V_{OC}^{Auger-limit} &<< V_{OC}^{Radiative} \quad \textit{(reflecting back surface)} \\ V_{OC}^{Auger-limit} &\approx V_{OC}^{Radiative} \quad \textit{(absorbing back substrate)} \end{aligned} \quad (7)$$

SURFACE-LIMITED OPEN-CIRCUIT VOLTAGE

Bulk-defect and surface recombination provide an additional and often dominant carrier recombination path that acts in parallel with the radiative and Auger processes above. Defect recombination reduces the generated electrochemical potential energy below the intrinsic Auger limit. Equation (8) gives the approximate expression for the surface recombination rates according to general semiconductor Shockley–Read-Hall theory [15]. The asymptotic solutions (neglecting Auger and radiative losses) for the surface-limited open-circuit voltage are given in equation (9) and (10) for both the low-level (LLI) and high-level injection (HLI) regimes:

$$U_{Surface} = \frac{np}{(p + p_1)/S_n + (n + n_1)/S_p} \quad (8)$$

$$V_{OC}^{Surface-LLI} = \frac{kT}{q} ln\left(\frac{J_L}{q\frac{n_i^2}{N_D} S_p + q\frac{n_i^2}{N_A} S_n}\right) \quad , \quad V_{OC}^{Surface-HLII} = 2\frac{kT}{q} ln\left(\frac{J_L}{q n_i (S_n + S_p)}\right) \quad (9\text{-}10)$$

Where S_n and S_p are the surface recombination velocities for electrons and holes respectively, and p_1 and n_1 depend on the energy level of the defect (assumed here to be mid-gap levels) and represent the equilibrium hole and electron concentrations that would result if the Fermi level coincided with the defect level. The requirements for surface recombination velocity (assuming $S_n = S_p$) to maintain the intrinsic Auger-limited open-circuit voltage are approximated as (where N_B is the background doping):

$$S^{low-injection} << WC_P N_B^2 \quad , \quad S^{high-injection} << \left[\frac{J_L^2 (C_n + C_p) W}{q^2} \right]^{1/3} \qquad (11\text{-}12)$$

Similar expressions for bulk Shockley Read Hall recombination due to mid-gap defect states yield requirements on the bulk Shockley Read Hall lifetime to maintain the intrinsic Auger-limited V_{OC}[8].

$$t^{low-injection} >> 1/C_p N_B^2 \quad , \quad t^{high-injection} >> \left[q^2 W^2 / J^2 (C_P + C_n) \right]^{1/3} \qquad (13\text{-}14)$$

Equations (12) and (14) indicate that for light injection currents under consideration, the interface recombination velocity and bulk defect lifetimes needs to be less than 200 cm/s and greater than 1 µs respectively to approach the high-level injection Auger limit. Unlike Auger recombination, there is no conceptual bound to the minimum value of interface recombination velocity ($S \geq 0$) or bulk defect recombination, but rather the practical difficulty of achieving such high quality material.

NUMERICAL SIMULATIONS

Numerical simulations of the semiconductor continuity equations using PC-1D version 5.5, a commercial photovoltaic simulator, were used to cross-check the limiting behaviors and physics discussed in sections 2.1-2.3. The numerical simulator eliminates many of the simplifying assumptions used above, and calculates the device electrical characteristics when all competing processes occur in parallel. The simulator does not calculate photon recycling; however this can be accounted for by specifying the corrected radiative coefficient (B/φ) for the appropriate optical boundary conditions, diode thickness, and absorptivity.

Figure 2 shows predicted efficiency and power density as a function of Auger coefficient with a back surface reflector at three diode temperatures between 27 °C and 100 °C assuming the same spectral performance in section 2.0 (above-bandgap light not absorbed in the diode but reflected by the BSR is conservatively not accounted for in the spectral efficiency). Auger-limited diodes with minimal defects operating in high-level injection (solid markers) are compared to diodes with typical parasitic interface and defect recombination (open markers). The lightly shaded blue region shows the region where best estimates for Auger coefficients in 0.52 eV InGaAsSb exist.[9] The curves illustrate that an aggressive limit to 0.52 eV InGaAsSb TPV thermal-to-electric conversion efficiency is 30% with a power density of ~0.9 W/cm^2 for near room temperature operation. For diode temperatures of 100°C the efficiency limit drops from 30% to ~20%, with a corresponding decrease in power density, and is due primarily to reduced open-circuit voltage.

Figure 3 shows the parametric numerical simulation of the diode open-circuit voltage as a function of P-type acceptor doping for several different interface recombination velocities with and without a perfect back surface reflector. The predicted behavior and limiting magnitudes agree with the simplified expressions discussed in sections 2.1-2.3. In high-level injection ($N_A < 10^{17}$ cm^{-3}) the Auger-limited voltage is ~370 mV, however as the surface recombination increases beyond 100 cm/s, the voltage becomes severely degraded and follows the predicted behavior of equations (11) and (12). In low injection ($N_A > 10^{17}$ cm^{-3}) the voltage changes according to equations (5) and (9) depending on whether the device is Auger-limited or surface limited. As seen in Figure 3b the presence of an absorbing back surface reduces the maximum open-circuit voltage below the Auger-limit due to the approximate order of magnitude increase in radiative flux emitted by the diode (i.e., reduced photon recycling).

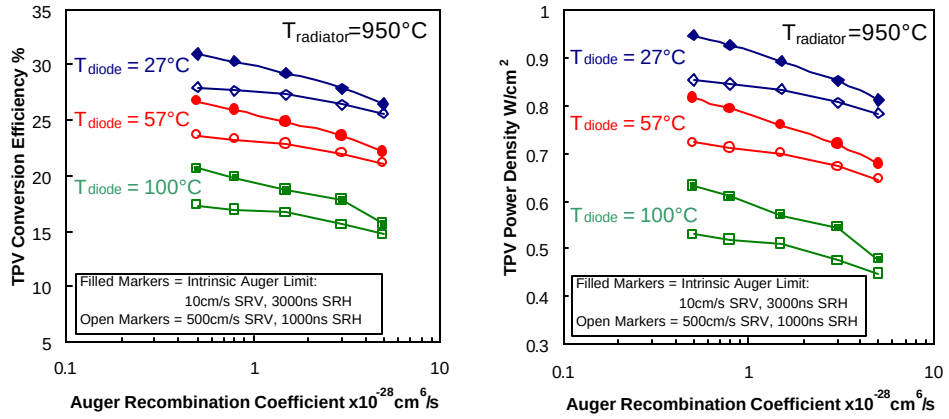

FIGURE 2. The predicted efficiency limits of 0.52eV InGaAsSb TPV diodes having effective photon recycling (i.e. designs having a back surface reflector) and high material quality, will ultimately be limited by Auger recombination. Assuming the front surface spectral control shown in Figure 1, Figure 2 shows the projected thermal to electric conversion efficiency and power density for three different diode temperatures having 10% grid shading and a radiator emissivity of 0.9. The performance projections are plotted as a function of Auger recombination coefficient and are shown for negligible bulk and interface recombination (solid markers) and for state-of-the-art material parameters (open markers). The shaded blue band illustrates a range of Auger coefficients recently reported in the literature for ~0.5eV III-V diodes [9,10].

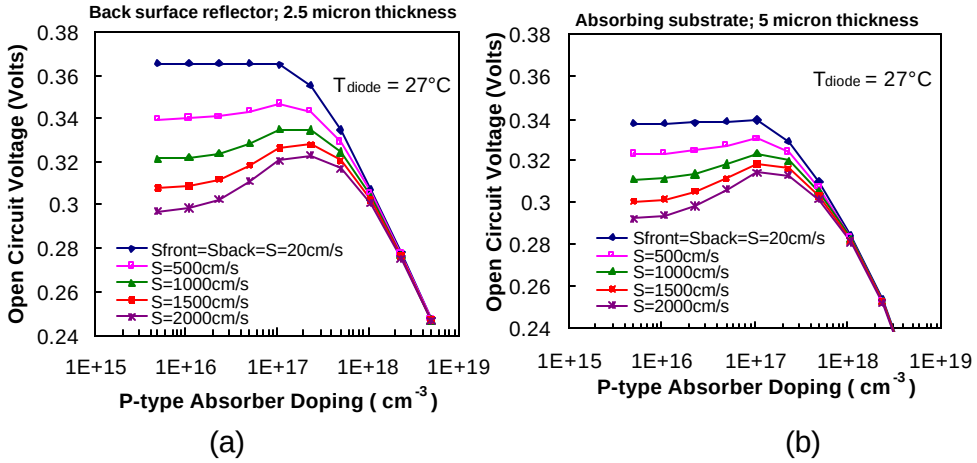

(a) (b)

FIGURE 3. (a) Simulated dependence of open circuit voltage as a function of background hole concentration in the p-type absorber for a two-pass photon recycled TPV architecture having a back surface reflector for different values of surface/interface recombination velocities (left hand figure). (b) The right hand figure again shows the open circuit voltage as a function of background hole concentration in the p-type absorber however for a single pass architecture (perfectly absorbing substrate/back contact). The significantly higher obtainable voltages in the two-pass architecture are enabled by (i) the reduction in volume and (ii) recycling of radiative recombination energy within the active diode region.

MINORITY CARRIER LIFETIME MEASUREMENTS

P-type InGaAsSb is chosen for the thick absorbing region and is therefore the largest contribution to the total diode recombination. Recent time-resolved photoluminescence decay and RF photoreflectance measurements, have empirically determined many of the decay coefficients in P-type InGaAsSb material. Table I summarizes the results:

Table I indicates that p-type InGaAsSb material quality exhibits good Shockley-Read-Hall lifetimes, and that recent improvements to heterojunction interface quality has reduced the surface recombination velocity to less than 100 cm/s. Very little data currently exists for n-type 0.52eV InGaAsSb material.

Table I. Summary of recombination coefficients in P-type InGaAsSb

Recombination Coefficient	Value	Reference
Auger Coefficient	$C = 1\times10^{-28}$ cm^6/s	[9]
Radiative Coefficient	$B=1.5\times10^{-10}$ cm^3/s	[19]
Shockley Read Hall Lifetime	$\tau_{SRH} \sim 1\mu s$	[18,20]
Interface Recombination Velocity	GaSb passivation ~1000-2000 cm/s AlGaAsSb passivation ~700 cm/s AlGaAsSb passivation, no growth interrupt < 100cm/s	[20] [21]

DIODE ELECTRICAL PROPERTIES

Various architecture 0.52eV InGaAsSb TPV diodes have been grown by MOCVD at both MIT Lincoln Laboratories and Sarnoff Corporation including shallow emitter N/P and thick emitter P/N architectures, see Figure 4. In both cases GaSb (E_g = 0.74eV) and AlGaAsSb (E_g = 1.0eV) heterojunction interface passivation has been investigated with the observation that the AlGaAsSb confinement provides the highest open-circuit voltage, which is in agreement with modeling and minority carrier lifetime measurements. Both devices with AlGaAsSb passivation on the p-type absorber measure room temperature dark current densities of approximately 1×10^{-5} A/cm^2 with near unity ideality, whereas devices with GaSb p-type confinement have approximately 2x the dark current densities. Currently, the device performance is insensitive to the choice of confinement on the n-type side. Low (< 10 mΩ) series resistance and good fill factors of ~70% are routinely observed for both P/N and N/P architectures.

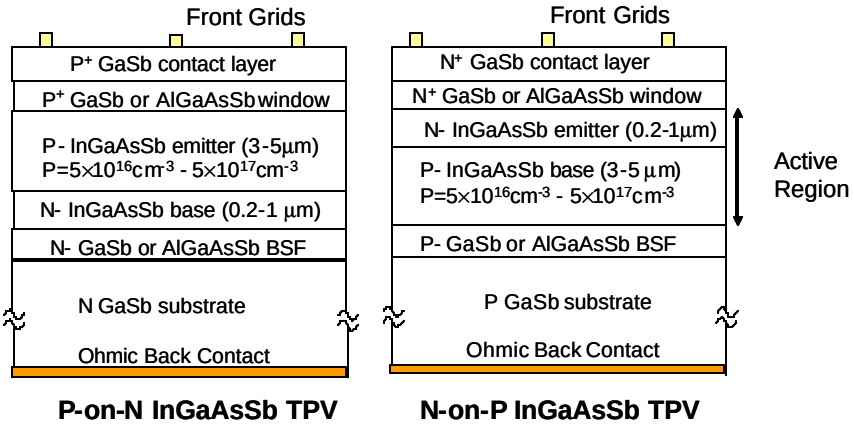

FIGURE 4. Typical P-on-N and N-onP InGaAsSb TPV diode architectures on GaSb substrates.

P/N STRUCTURES

The P/N architecture has been the baseline device architecture for a number of years. Figure 5a shows the V_{oc}-J_{SC} relation measured for various illumination intensities of three different diodes with various lattice-matched caps and back surface passivation (AlGaAsSb and GaSb). The slope and magnitude of the curve gives the ideality and dark current density respectively, which in general vary with illumination level. The lowest dark currents are measured with p-type AlGaAsSb interface passivation, however the diode's dark current appears to be insensitive to whether the n-type passivation material is GaSb or AlGaAsSb. Three different simulated dark currents are also shown in the figure for diodes having $C = 1\times10^{-28}$cm^6/s, τ_{SRH} = 1 μs, and: (i) An absorbing back surface and S = 1000 cm/s, (ii) an absorbing back surface and S = 20 cm/s and (iii) a reflecting back surface and S = 20 cm/s. The simulated dark current density in case (iii) approaches the high-level injection Auger-limited open-circuit voltage. The simulations show the expected gains in diode open-circuit voltage with improvements in photon recycling and minimizing defect recombination. The lowest measured room temperature dark current is 1.4×10^{-5} A/cm^2 with an ideality of ~1.1 for diodes with p-type AlGaAsSb passivation; P/N

diodes with P-type GaSb passivation show room temperature dark current of 2.5×10^{-5} A/cm^2 with an ideality of ~1.0. Diodes measured were all 0.5 cm^2.

N/P STRUCTURES

Shallow emitter N/P structures have been enabled by the development of low-temperature annealed shallow contacts to n-type GaSb.[22], whereas the p-type contact is simply made to the p-type GaSb substrate. Figure 5b shows the V_{oc}-J_{SC} relation measured for various illumination intensities of three different diodes with various lattice-matched caps and back surface passivation (AlGaAsSb and GaSb). Similar to the P/N structure the lowest dark currents are measured with p-type AlGaAsSb regardless of either GaSb or AlGaAsSb n-type passivation. The same 3 simulation cases as in the P/N structures are also shown in the figure. As before, the simulations show expected gains in diode open-circuit voltage with improvements in photon recycling and material quality. The lowest measured room temperature dark current for p-type AlGaAsSb passivation is similar to the P/N architecture at ~1.5×10^{-5} A/cm^2 with an ideality of ~1.1. Interestingly, N/P diodes with P-type GaSb passivation show significantly higher room temperature dark current; based on the preliminary nature of the N/P development the origin of this large increase is not understood. Diodes measured were all 0.5 cm^2.

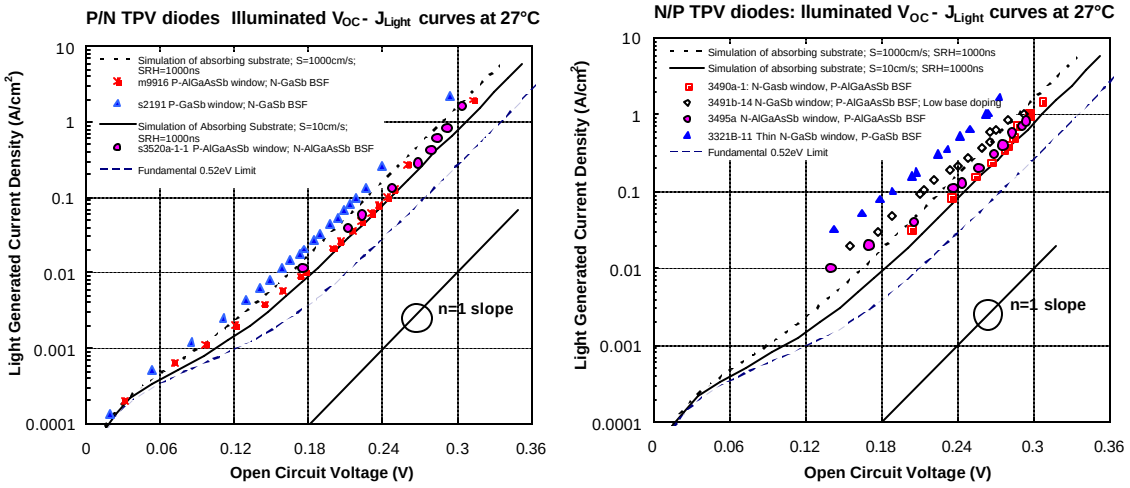

(a) (b)

FIGURE 5. Variable illumination short circuit current density vs. open circuit voltage characteristics for various P-on-N ((a) left hand side) and N-on-P ((b) right hand side) diode architectures on GaSb substrates.

Table II. Summary of normalized voltage factors for P/N and N/P architectures using various front surface and back surface passivation materials.

InGaAsSb Architecture	Front surface passivation	Back Surface Field	E_{Gap} (10% of EQE)	V_{oc} @ 1A/cm^2	Voltage Factor at 1A/cm^2
P/N #s2191	GaSb	GaSb	0.522eV	276mV	**53%**
P/N #m9916	AlGaAsSb	GaSb	0.527eV	295mV	**56%**
P/N #s3520	AlGaAsSb	AlGaAsSb	.527eV	295mV	**56%**
N/P #s3321	GaSb	GaSb	0.524eV	260mV	**50%**
N/P #s3491	GaSb	AlGaAsSb	0.527	295mV	**56%**
N/P #s3495	AlGaAsSb	AlGaAsSb	.527	292mV	**56%**

SUMMARY OF DEVICE ARCHITECTURES

Table II summarizes the open-circuit voltage data and quantum efficiency cutoff wavelengths for the samples shown in Figures 4-5. The open-circuit voltage is normalized to its value at 1A/cm^2, and would be greater at expected current densities of ~3 A/cm^2. As mentioned previously N/P and P/N architectures exhibit equivalent dark currents and voltage factors using p-type AlGaAsSb confinement with no distinction between AlGaAsSb or GaSb confinement of n-type material. Here, the voltage factor is the ratio of open circuit voltage divided by the QE cutoff energy. With material improvements and a reflecting back surface, voltage factors are predicted to increase to approximately 66% (J_L = 1 A/cm^2) and 70% (J_L = 3 A/cm^2) near the high-level injection Auger limit, representing nearly a 20% improvement.

BACK SURFACE REFLECTORS

As discussed in Section 2, incorporating a reflecting back surface in the TPV architecture is needed to realize the maximum voltage. In this section, preliminary results on back surface reflector InGaAsSb TPV diodes utilizing epoxy bonding and total substrate removal are presented[23,24]. Figure 6 shows the schematic for a device fabricated by bonding with transparent epoxy a grid patterned N/P InGaAsSb TPV diode to a GaSb handle substrate, which has a pre-deposited gold reflector. The reflector is gridded and allows for a partial ohmic contact for ~10% of the surface area and a highly reflective surface for the remaining ~90%. After bonding, the original GaSb substrate was removed via lapping and selective chemical etching to an InAsSb stop etch layer[23]. After stop etch removal, front grids were deposited on the epitaxial layer.

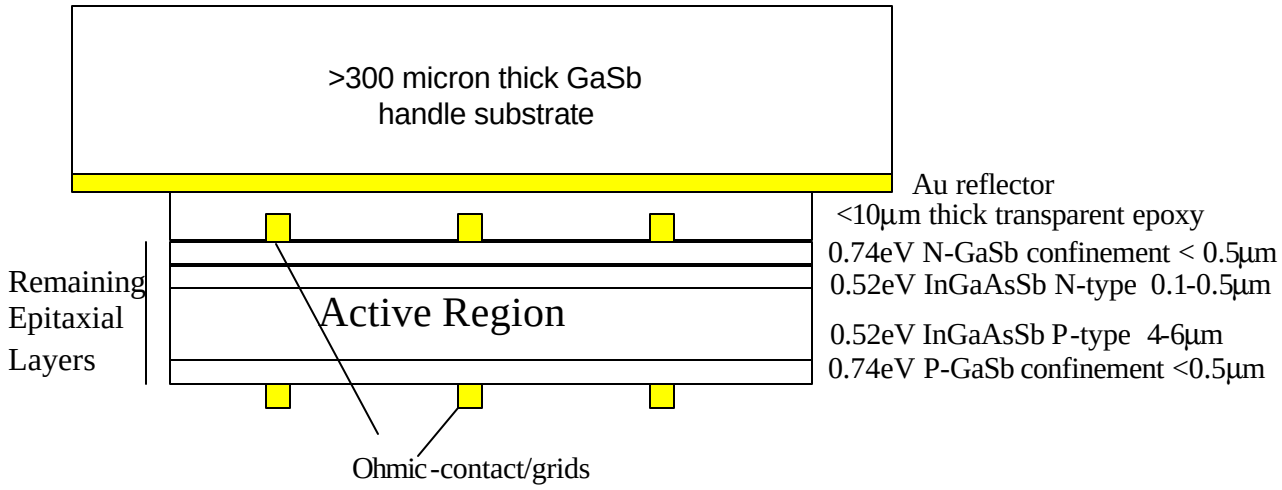

FIGURE 6. Wafer transferred TPV diode architecture with full substrate removal and back surface reflector

The device was tested under various illumination conditions, see Figure 7a. The device's soft electrical characteristics indicate poor fill factor, due to a high series resistance probably due to contact adhesion problems, and possibly some shunting of the device due to damage during the processing. Despite these flaws, the initial devices exhibit good open-circuit voltages under low/medium illuminations as exhibited by the J_{SC} versus V_{OC} curves, see Figure 7b, which also indicate a high ideality of approximately 2. Care must be taken when drawing conclusions from Figure 7 since the parasitic resistance introduced during processing may obscure the undamaged diode behavior. Unfortunately, further testing is not possible as the devices were damaged during testing at high currents during calibration.

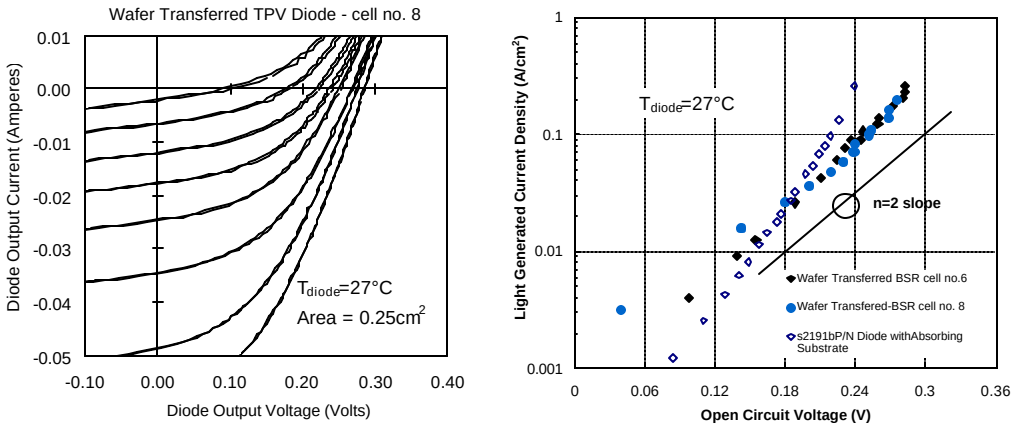

FIGURE 7. Current-voltage characteristics of wafer transferred back surface reflector devices

IN-CAVITY MEASUREMENTS

The performance of a small TPV module using P/N 0.52eV InGaAsSb TPV diodes has been measured in a prototypic test cavity. Efficiency in this test was calculated as the ratio of peak module electric power to total module heat absorption rate. These parameters were measured simultaneously to assure validity of the final efficiency value. Modules were built with both a 1 cm^2 and 4 cm^2 area structure composed of two and eight cells, each 0.5 cm x 1.0 cm. A front surface filter[11] is joined to both modules with epoxy. The photonic cavity is prototypical of a flat-plate TPV generator design, where the radiator is a large flat silicon carbide surface. The TPV module was fixed to the top of a copper pedestal to facilitate heat absorption measurements. The test was run in vacuum to eliminate conductive and convective heat transfer. Reference [24] gives details of the test apparatus.

The photonic cavity provides an optimal test environment for TPV efficiency measurements because it incorporates all known phenomena found in a practical operating TPV system, such as: non-ideal radiator emissivity, full radiator spectral and angular dispersion, photon recycling, and complex module geometry.

Repeatable measurements yield a conversion efficiency of ~18-19% at a radiator temperature of 950 C and diode temperature of 27 °C using 0.52eV InGaAsSb TPV diodes with front surface spectral control. Figure 8 shows the measured efficiency and power density versus radiator and diode temperature.

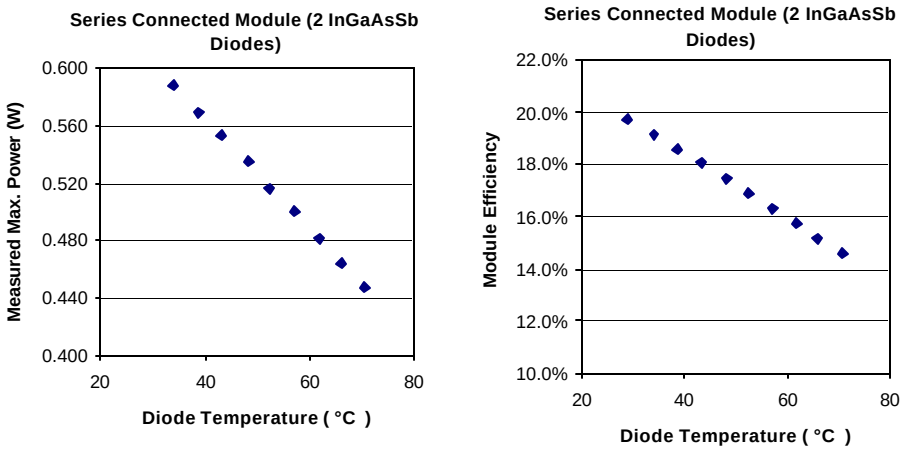

FIGURE 8. Measured in-cavity thermal to electric conversion efficiency of nearly 20% have been measured at radiator temperatures of 950°C and diode temperatures of 27°C for both 1cm^2 (shown) and 4cm^2 modules. Diodes used in the modules are the P-on-N architecture on GaSb substrates, using a mix of both p-type GaSb and AlGaAsSb confinement. Figure 11 shows the measured efficiency and power density as a function of diode temperature.

SUMMARY

Small scale TPV modules (4cm^2) having InGaAsSb TPV diodes integrated with front surface filters have demonstrated 19% thermal-to-electric efficiency and ~0.55W/cm^2 power density for hot side temperatures of 950°C and diode temperature of ~25°C. Near term improvements of a few absolute percent are expected by incorporating improvements in interface recombination velocity into diodes used in the module. Potential for nearly 30% efficient conversion efficiency (~0.9W/cm^2) will require (i) aggressive processing techniques and (ii) InGaAsSb material/interface quality improvements to incorporate a suitable back surface reflector and to reduce parasitic absorption and non-radiative recombination. Further characterization of the n-type InGaAsSb material/interfaces is required to determine how/if this layer contributes significantly to the total dark current.

REFERENCES

[1] P.F. Baldasaro, J.E. raynolds, G.W. Charache, D.M. Depoy, C.T. Ballinger, T. Donovan, and J.M. Borrego, J. Appl. Phys., vol. 89, pp. 3319-3327, (2001).

[2] B. Wernsman, R.R. Siergiej, S.D. Link, R.G. Mahorter, M.N. Palmisiano, R.J. Wehrer, R.W. Shultz, R.L. Messham, S. Murray, C.S. Murray, F. Newman, D. Taylor, D. Depoy, and T. Rahmlow, IEEE Trans. Elec. Dev., vol. 51, no. 3, pp. 512-516, (20004).

[3] R. J. Wehrer, M.W. Wanlass, D. Taylor, B. Wernsman, J.J. Carapella, R.W. Schutlz, S. P. Ahrenkiel, D.M. Wilt, M.W. Dashiell, R.R. Siergiej, and S.D. Link, "0.52eV InGaAs/InPAs ThermoPhotoVoltaic Cells", See these proceedings

[4] G.W. Charache, P.F. Baldasaro, L.R. Danielson, D.M. Depoy, M.J. Freeman, C.A. Wang, H.K. Choi, D.Z. Garbuzov, R.U. Martinelli, V. Khalfin, S. Saroop, J.M. Borego, InGaAsSb therophotovoltaic diode: Physics Evaluation, J. Appl. Phys., vol. 85, pp. 2247-2252, (1999).

[5] C.A. Wang, H.K. Choi, S.L Ransom, G.W. Charache, L.R. Danielson, and D.M. Depoy, Appl. Phys. Lett., 75, pp. 1305-1307, (1999)

[6] C.W. Hitchcock, R.J. Gutmann, J.M. Borego, I.B. Bhat, G.W. Carache, IEEE Trans. Electr. Devices, vol. 46, no. 10, pp. 2154-2161 (1999).

[7] Tom Tiedje, et al., IEEE Transactions on Electron Devices, vol. ED-31, pp. 711-716, (1984)

[8] Martin A. Green, IEEE Transactions on Electron Devices, vol. ED-31, pp. 671-678, (1984)

[9] S. Anikeev, D. Donetski, G. Belenki, S. Luryi, C.A. Wang, J.M. Borrego, G. Nichols, "Measurement of the Auger Recombination rate in p-type 0.54eV GaInAsSb by time-resolved photoluminescence", to be published in Applied Physics Letters.

[10] W. Metzger, M.W. Wanlass, R.J. Ellingson, R.K. Ahrenkiel, and J.J. Carapella, "Auger Recombination in low-bandgpa n-type InGaAs", App. Phys. Lett.,

[11] T.D. Rahmlow, "Design Considerations and Fabrication Results for Front Surface TPV Spectral Control Filters", See these proceedings.

[12] H.K. Choi, C.A. Wang, G.W. Turner, M.J. Manfra, D.L. Spears, G.W. Charache, L.R. Danielson, and D.M Depoy, Appl. Phys. Lett., 71, pp. 3758-3760, (1997)

[13] W. Shockley and H.A. Queisser, J. Appl. Phys., vol. 32, pp. 510, (1961)

[14] C. H. Henry, J. Appl. Phys., vol. 51, pp. 4494-4500, (1980).

[15]. S.M. Sze, "Physics of Semiconductor Devices", 2nd Edition, John Wiley and Sons, Inc. 1981.

[16] W. van Roosbroeke and W. Shockley, Physical Review, vol. 94, pp. 1558-1560, (1954).

[17] P. Asbeck, J. Appl. Phys., vol. 48, pp. 820-822, (1977).

[18] D. Donetski, "To be presented at the 12th ICMOVPE" Lahina, Hawaii, June 2004

[20] D. Donetski, , S. Anikeev, G. Belenky, S. Luryi, C.A. Wang, G. Nichols, Appl. Phys. Lett., 81, pp4769-4771 (2002).

[21] C.A. Wang, "Effect of Growth Interuption on Surface Recombination Velocity in GaInAsSb/AlGaAsSb Heterostructures Grown by Organometallic Vapor Phase Epitaxy", "To be presented at the 12th ICMOVPE" Lahina, Hawaii, June 2004

[22] R. Huang, C.A. Wang, C.T. Harris, M.K. Connors, D.A. Shiau "Ohmic Contacts to n-type GaSb and n-type GaInAsSb", Accepted for Publication in Journal of Electronic Materials

[23] C. Wang, "Monolithically Series-Interconnected GaInAsSb/AlGaAsSb TPV devices wafer bonded to GaAs", see these proceedings

[24] C.K. Gethers, C.T. Ballinger, and D.M DePoy, in Thermophotovoltaic Generation of Electricity - 4th NREL Conference Proceedings, Denver CO, 1998, p. 335-348, AIP Proceedings 460.